Association of survival and disease progression with chromosomal instability: A genomic exploration of colorectal cancer

Association of survival and disease progression with chromosomal instability: A genomic exploration of colorectal cancer

Michal Sheffer[a,1], Manny D. Bacolod[b,1], Or Zuk[c], Sarah F. Giardina[b], Hanna Pincas[b], Francis Barany[b], Philip B. Paty[d], William L. Gerald[e,3], Daniel A. Notterman[f,2], and Eytan Domany[a,2,4]

[a]Department of Physics of Complex Systems, Weizmann Institute of Science, Rehovot 76100, Israel; [b]Department of Microbiology, Weill Medical College of Cornell University, 1300 York Avenue, New York, NY 10021; [c]Broad Institute, Massachusetts Institute of Technology and Harvard University, 7 Cambridge Center, Cambridge, MA 02142; Departments of [e]Pathology and [d]Surgery, Memorial Sloan-Kettering Cancer Center, 1275 York Avenue, New York, NY 10065; and [f]Department of Molecular Biology, Princeton University, Princeton, NJ 08544

Communicated by Thomas E. Shenk, Princeton University, Princeton, NJ, February 27, 2009 (received for review October 2, 2008)

During disease progression the cells that comprise solid malignancies undergo significant changes in gene copy number and chromosome structure. Colorectal cancer provides an excellent model to study this process. To indentify and characterize chromosomal abnormalities in colorectal cancer, we performed a statistical analysis of 299 expression and 130 SNP arrays profiled at different stages of the disease, including normal tissue, adenoma, stages 1–4 adenocarcinoma, and metastasis. We identified broad (> 1/2 chromosomal arm) and focal (< 1/2 chromosomal arm) events. Broad amplifications were noted on chromosomes 7, 8q, 13q, 20, and X and broad deletions on chromosomes 4, 8p, 14q, 15q, 17p, 18, 20p, and 22q. Focal events (gains or losses) were identified in regions containing known cancer pathway genes, such as *VEGFA*, *MYC*, *MET*, *FGF6*, *FGF23*, *LYN*, *MMP9*, *MYBL2*, *AURKA*, *UBE2C*, and *PTEN*. Other focal events encompassed potential new candidate tumor suppressors (losses) and oncogenes (gains), including *CCDC68*, *CSMD1*, *POLR1D*, and *PMEPA1*. From the expression data, we identified genes whose expression levels reflected their copy number changes and used this relationship to impute copy number changes to samples without accompanying SNP data. This analysis provided the statistical power to show that deletions of 8p, 4p, and 15q are associated with survival and disease progression, and that samples with simultaneous deletions in 18q, 8p, 4p, and 15q have a particularly poor prognosis. Annotation analysis reveals that the oxidative phosphorylation pathway shows a strong tendency for decreased expression in the samples characterized by poor prognosis.

colon cancer | DNA copy number | gene expression | SNP arrays

The development of colorectal cancer from normal epithelial cells through benign adenomas to malignant carcinomas and metastasis is a lengthy, multistep process, involving accumulation of mutations of key regulatory genes (1). Two forms of genetic instability are described in colon cancer. Samples displaying *C*hromosomal *IN*stability (*CIN*) comprise 85% of the cases, and the rest display *M*icrosatellite *In*stability (*MIN*)—deletions and amplifications of short sequences of nucleotides. MIN tumors are usually euploid, while CIN tumors are aneuploid; these genetic differences are reflected in a different pathological and clinical behavior (2). Numerous array comparative genomic hybridization (CG*H*) and SNP chip studies (3–5) (*SI References*) have shown that the principal large-scale DNA copy number changes in CIN-colorectal cancer are gains of chromosomes 7, 8q, 13q, and 20 and losses of 4, 8p, 17p, 18, and 20p.

Genomic aberrations that recur in many different samples may reflect an underlying selection advantage. Therefore, they often include genes that are important for tumor development, propagation, and spread (6). Tumor suppressor genes (TSG) are generally inactivated through mutation or deletion (generally of both copies) while oncogenes become active through mutation or amplification (generally of 1 copy). Tsafrir et al. (7) showed, contrary to previous claims (8), that changes in expression level were correlated with alterations in gene dose, suggesting that coherent transcriptional changes associated with large chromosomal segments can be attributed to corresponding changes in chromosome structure, such as copy number variation. They also showed that aberrations became more frequent as disease advanced.

Using novel methods of analysis and a much larger sample size than available to Tsafrir et al. (7), we planned to create a comprehensive map of the common genomic aberrations in colon cancer and identify the genes encompassed by these events. Data that were collected from patients at a variety of clinical stages allowed us to associate chromosomal changes with survival and disease progression and to identify genetic and biochemical pathways that are affected by these aberrations. Information from DNA copy number (from Affymetrix 50 k SNP arrays, see *Methods*) and gene expression (from Affymetrix U133A arrays) was integrated. First, we used the SNP data to identify amplification and deletion events that occur in a large subset of samples. We refer to these collectively as *CINons*. Next, data from tumor samples for which we had both copy number and expression were used to identify genes, the expression of which was significantly correlated with the copy number implied by their cognate SNPs. We term these "correlated genes" and focus our attention on them as potential cancer pathway candidates. Finally, we used the tumors with both SNP (i.e., copy number) and expression data to establish that for some CINons we can impute the copy number change of individual samples from the associated expression data. This allowed us to construct an in silico chromosomal alteration map for the much larger number of tumors for which only expression data were available. This procedure significantly enhanced the statistical power of our search for linkage between survival and amplifications/deletions. Ultimately, we identify several new candidate cancer pathway genes in colon cancer, and demonstrate a strong association between deletions of 18q, 8p, 4p, and 15q and outcome. This association may be related to reduced expression of genes annotated to the oxidative phosphorylation pathway.

Results and Discussion

Amplifications and Deletions in Colon Cancer (SNP Data). Fig. 1*A* shows the smoothed $CR_{n,s}$ (log copy number ratio for SNP n and

Author contributions: M.S., M.D.B., F.B., D.A.N., and E.D. designed research; M.S., M.D.B., S.F.G., H.P., F.B., P.B.P., W.L.G., D.A.N., and E.D. performed research; M.S., O.Z., and E.D. analyzed data; and M.S., D.A.N., and E.D. wrote the paper.

The authors declare no conflict of interest.

[1]M.S. and M.D.B. contributed equally to this work.

[2]E.D. and D.A.N. contributed equally to this work.

[3]Deceased September 14, 2008.

[4]To whom correspondence should be addressed. E-mail: eytan.domany@weizmann.ac.il.

This article contains supporting information online at www.pnas.org/cgi/content/full/0902232106/DCSupplemental.

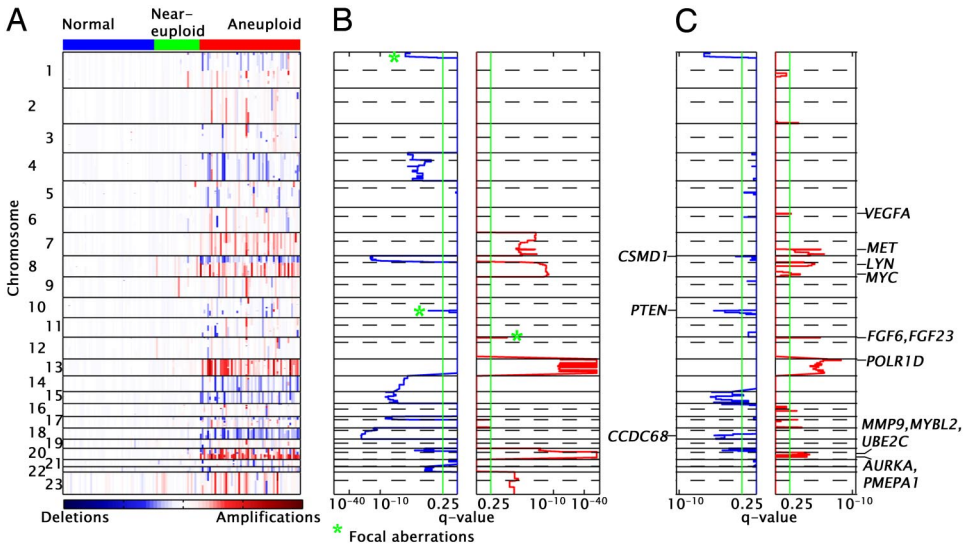

Fig. 1. Chromosomal instabilities in colon cancer. (*A*) Rows represent SNPs and columns represent samples. The colored entries represent the level of copy number changes with amplifications in red and deletions in blue. The values are the smoothed *log-copy number ratios* $CR_{n,s}$ (see *Methods*). The color bar at the *Top* of the figure identifies normal tissue (blue), near-euploid tumors (green), and aneuploid tumors (red). (*B*) The CINons found by the GISTIC method (configuration 1): the *Left* plot (blue trace) shows the $-\log(q\text{-values})$ for deletions and the *Right* plot (red trace) shows the $-\log(q\text{-values})$ for amplification (the *x* axis was scaled for visualization purposes). The CINons marked with green * are focal; the remaining are broad (see *Methods*). The dotted line separates the *p* and *q* arms of the chromosome. (*C*) Same as *b* for configuration 2 (see *Methods* and *SI Methods*).

sample *s*, see *Methods*) values obtained from the SNP data. The samples are divided into 3 groups: normal, marked blue in *Top* color bar (50 samples); near-euploid (green), mainly MIN tumors (25 samples); and aneuploid (red), CIN tumors (55 samples).

We implemented the Genomic Identification of Significant Targets in Cancer (GISTIC) algorithm (9) to identify statistically significant amplifications and deletions. The results displayed in Fig. 1 are for the 55 tumors with high levels of aneuploidy; adding the 25 near-euploid tumors gave nearly identical results. Using the initial set of parameters (referred to as configuration 1; see *Methods* and *SI Methods*), we identified 18 *broad* and 3 *focal* events (CINons). The location of each CINon, and the corresponding position-dependent statistical significance of the aberration (*q*-value, see *Methods*), is shown in Fig. 1*B*.

We hypothesize that within a CINon, the so-called "driver mutation" (9), which provides a selective advantage to individual tumors, is located in the SNP regions ("peaks") associated with the minimal *q*-values. Some CINons have minimal *q*-values across a large region of the chromosome, making it impossible to locate and identify potential driver mutations (see Fig. 1*B*). To overcome this problem, we repeated the GISTIC analysis using a different configuration (*configuration 2*, see *Methods* and *SI Methods*). This approach uncovered both additional focal events (see Table 1) that had been subsumed within the signal of the broad amplifications and deletions and narrower *q*-value minima within these previously identified broad events (Fig. 1*C*). These additional *q*-value minima are termed, "peak events" or "peak CINons." Of importance, several peak CINons identified in this fashion contain previously established cancer pathway genes. Table 1 presents all of the broad, focal, and peak events that we found using both *configurations 1* and *2*, and the proportion of tumor samples that carry each. Of the 18 broad CINons (see Fig. 1 and Table 1) 8 are amplifications on chromosomes 7p, 7q, 8q, 13q, 20p, 20q, Xp, and Xq, and 10 are deletions on chromosomes 4p, 4q, 8p, 14q, 15q, 17p, 18p, 18q, 20p, and 22q. Most of these broad CINons were previously described (3–5, *SI References*).

We also found 10 focal CINons; amplifications on 2q, 6p, 8p (part of the 8q broad amplification), 12p, 16q, and 2 on 17q and deletions on 1p, 10q, and 16p. Finally, 17 peak CINons were identified.

Identifying Correlated Genes. To establish the relationship between copy number changes and gene expression, we identified the U133A expression microarray probe sets ("expressed genes") that mapped to each CINon detected with the SNP array and computed the Pearson correlation coefficient (PCC) between the associated expression level and copy number (see *Methods*). A list of significantly correlated "expressed genes" was assembled; the number of such probe sets for every CINon is also presented in Table 1. For some peak CINons, no (or very few) correlated gene was found, but in most cases there were more than 5 and for some broad CINons there were more than 100. Although statistically significant amplifications or deletions that carry no correlated expressed gene are intriguing because they may contain important regulatory elements or express noncoding RNA, we focused our attention on the genes whose mRNA expression was significantly correlated to their copy number.

Cancer Pathway Genes Significantly Correlated with Broad and Focal Events. *Focal CINons:* The amplification on 6p contains *VEGFA*, a growth factor active in angiogenesis, vasculogenesis, and endothelial cell growth (10). 12p contains *FGF6* and *FGF23*, members of the fibroblast growth factor (*FGF*) family, which mediate a variety of cellular responses during embryonic development and in the adult organism and play an important role in tumor angiogenesis (11) (the fact that we did not detect expression of these *FGF* genes, even though they reside on an amplified segment, may be caused by poor performance of the relevant expression array probe sets). The focal deletion on 10q contains *PTEN*, a TSG that antagonizes the *PI3K-AKT* signaling pathway. *PTEN*, known to be deleted or mutated in many types of cancers (12), is located on 10q23, a genomic region that suffers loss of heterozygosity (*LOH*) in cancer.

Peak CINons contain several known oncogenes: *MYC* (8q24.21), a transcription factor for growth-related genes, is often amplified and overexpressed in colorectal cancer (13). *LYN* (8q12.1) is a *SRC* kinase normally involved in B-cell signaling and cellular proliferation, differentiation, and migration. Interestingly, *LYN* appears to be a component in the pathway by which *CD44* regulates *AKT* phosphorylation and inhibits apoptosis. Thus amplification of *LYN* and deletion of *PTEN* could have synergistic growth-promoting effects on the *AKT* signaling pathway. Furthermore, upregulation has been associated with resistance to chemotherapy (14, 15). The proto-oncogene *MET* (7q31.2), a growth factor receptor required for embryonic development, is implicated in tumorigenesis, particularly in the development of invasive and metastatic phenotypes (16). The peak amplification on 20q13.12 contains several oncogenes: *MMP9*, a matrix metalloproteinase, known to facilitate local tumor spread and metastasis by promoting matrix degradation and cell migration (17); *MYBL2*, a transcription factor involved in regulation of progression through cell cycle and antiapoptosis (18); *UBE2C*, a ubiquitin-conjugating enzyme, is significantly overex-

Table 1. Broad, focal, and peak CINons found by the 2 configurations of GISTIC

Id	Chr		Start, Mb	End, Mb	Type	Samples, %	Noncoding RNA	Correlated* probe sets	Known and candidates oncogenes/TSG
1	2	q37.1	235.26	241.53	Focal	27	1	6/25	
2	6	p21.1	42.43	45.06	Focal	22	1	21/35	VEGFA
3	7	p	1.50	57.85	Broad	53	11	72/156	
4	7	q	61.71	158.75	Broad	42	22	157/355	
5	7	q31.2	115.92	116.13	Peak in 4	42	0	1/5	MET
6	7	q36.1	147.56	148.10	Peak in 4	44	0	2/3	
7	8	p	40.65	43.31	Focal	33	1	6/20	
8	8	q	47.40	143.90	Broad	56	12	111/216	
9	8	q11.22	52.31	59.16	Peak in 8	51	1	11/18	LYN
10	8	q24.13	125.01	130.59	Peak in 8	60	0	8/9	MYC
11	12	p13.32	4.33	4.76	Focal	18	0	2/7	FGF6, FGF23
12	13	Q	18.35	114.05	Broad	73	14	121/206	
13	13	q12.2	27.13	27.25	Peak in 12	78	0	1/1	POLR1D
14	16	q12.1	50.21	51.37	Focal	18	0	0/3	
15	17	q11.1	22.51	23.09	Focal	29	0	0/3	
16	17	q25.3	73.52	78.18	Focal	31	2	21/55	
17	20	p	0.10	26.15	Broad	47	8	46/93	
18	20	q	29.31	62.34	Broad	91	22	143/209	
19	20	q12–13.12	40.46	44.42	Peak in 18	93	0	22/40	MMP9, MYBL2, UBE2C
20	20	q13.2	53.72	58.44	Peak in 18	91	3	14/23	AURKA, PMEPA1
21	X	p	2.83	57.46	Broad	35	14	62/174	
22	X	q	62.48	154.50	Broad	38	63	67/265	
23	1	p	0.84	40.29	Focal	36	19	91/309	
24	1	p36.22	11.21	31.08	Peak in 23	36	9	50/157	
25	4	p	0.40	48.61	Broad	27	8	38/117	
26	4	q	52.38	190.95	Broad	25	14	88/304	
27	8	p	0.18	43.23	broad	58	9	58/153	
28	8	p23.2	5.76	6.25	Peak in 27	60	0	0/1	CSMD1
29	10	q23.31	89.89	90.21	Focal	20	0	1/2	PTEN
30	14	q	19.30	106.31	Broad	35	102	164/359	
31	15	q	19.92	100.18	Broad	42	97	109/342	
32	15	q11.2	21.60	23.67	Peak in 31	44	76	1/6	
33	15	q21.3	55.12	56.98	Peak in 31	45	0	3/10	
34	15	q26.2	93.07	93.08	Peak in 31	40	0	1/2	
35	16	p13.3	6.16	7.18	Focal	9	0	0/1	
36	17	p	0.45	22.05	Broad	47	24	73/177	
37	18	p	0.15	15.07	Broad	56	0	26/46	
38	18	q	16.84	75.59	Broad	71	10	55/111	
39	18	q21.2	50.79	50.99	Peak in 38	73	0	1/2	CCDC68
40	20	p	0.10	19.29	Broad	22	7	37/74	
41	20	p13	0.10	4.42	Peak in 40	22	6	20/36	
42	20	p12.1	14.45	14.80	Peak in 40	25	0	0/1	
43	20	p12.1	15.20	15.85	Peak in 40	22	0	1/2	
44	20	p12.1	17.74	19.29	Peak in 40	20	1	5/9	
45	22	q	15.51	49.02	Broad	24	14	51/266	

CINons 1–22 are amplicons and 23–45 deletons. The broad CINons (including the focal CINon 7, see text) were identified by configuration 1, the focal CINons 11, 23, and 29 were identified by both configurations, and the rest by configuration 2. *, see *Methods*.

pressed in many different types of cancers, and is associated with the degree of tumor differentiation in different types of carcinomas (19). Another peak amplification, on 20q13.2, contains *AURKA*, a serine/threonine kinase known as a key regulator of the mitotic cell division process, which has been identified as an oncogene overexpressed in many human cancers (20).

Candidate Cancer Pathway Genes Correlated with Broad and Focal Events. Some of the focal and peak CINons that we found contained candidate cancer pathway genes not previously known to play a role in colon cancer (a list of the correlated genes in these CINons is found in Table S1). One such candidate gene is *CCDC68* (18q21.2), also termed cutaneous T cell lymphoma-associated antigen se57–1. The role of *CCDC68* in cancer is not known. In colon cancer, *CCDC68* is expressed on the cancer cell surface in about 15% of patients (21). In our data this gene is downregulated in 89% of primary tumors (compared with normal tissue) and its expression is highly correlated with the associated gene copy number ($r = 0.51$; $P = 3.6e\text{-}5$). These observations suggest that downregulation of this surface protein is an important selective advantage for colon cancer cells and that it should be studied as a potential TSG. *CCDC68* is the gene closest to the peak deletion identified on chromosome 18 (Fig. 1*C*), which is also close to *DCC*, a known TSG in colon cancer, whose expression level was absent in our samples. *CSMD1*, located near the peak of the 8p deletion (8p23.2), is not represented on the microarray. Farrell et al. (22) also suggested this gene as a candidate TSG inactivated in colon cancer.

Several candidates are located in amplified regions and are overexpressed. *PMEPA1*, located on 20q13.31, is an androgen-induced gene expressed in normal prostate tissue. The role of *PMEPA1* in cancer is unclear because it shows overexpression in some colon, breast, and ovarian cancers but is underexpressed in prostate cancer. *PMEPA1* is known to be induced by the *TGF-β* signaling pathway, *EGF*, *IGF*, and *PDGF* (23), and it serves to inhibit *TGF-β* signaling by interfering with *TGF-β* type I receptor (*TGFBRI*)-induced *R-Smad* phosphorylation. Because *TGF-β* mediates an apoptotic pathway in colon cancer, the effect of *PMEPA1* overexpression could be to promote cancer cell growth by fore-

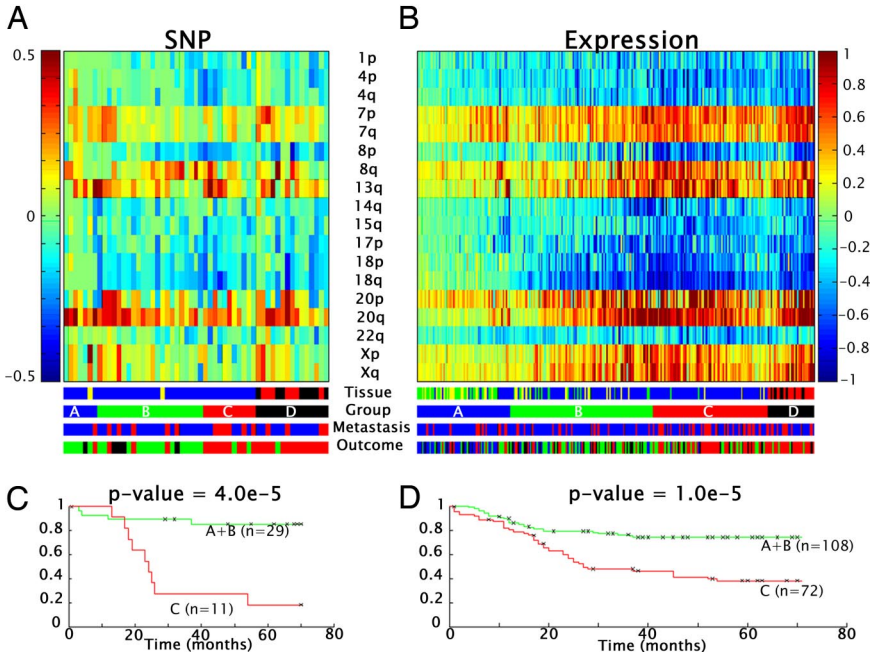

Fig. 2. CINon copy number tables, from SNP and expression. (A) Copy number table of the broad CINons (including the focal CINon 1p) as obtained from SNP data, for 55 aneuploid tumors; each row represents a broad CINon and each column a sample. An entry is calculated as the median of $CR_{n,s}$: the SNPs within the CINon, in the corresponding sample (see color bar to *Right* of figure). (*B*) CINon expression table, for 256 adenomas and tumors, similar to the copy number table (*A*). The entries were calculated as the median of the ''correlated genes'' of the CINon (see text and *Methods*). In both *a* and *b* the samples are divided into 4 groups as shown in the second color bar at the *Bottom* (in the text); the first color bar represents the tissue origin of the sample where primary tumor is blue, MIN tumor is yellow, adenoma is green, sample from liver metastasis is red, and sample from lung metastasis is black; in the third color bar the stage 4 tumors (primary samples presenting with metastasis) are in red; the fourth color bar represents outcome, where adenomas are in blue, good outcome samples in green, poor outcome in red, and unknown outcome in black. (*C* and *D*) Kaplan-Meier plot of primary tumor samples that belong to groups A + B (green) versus group C (red) of copy numbers and expression, respectively. Follow-up intervals that were greater than 70 months were assigned 70.

stalling apoptosis. In our data set, *PMEPA1* is overexpressed in 84% of the primary tumors (> 2-fold). Expression of *PMEPA1* exhibits high correlation with the associated copy numbers ($r = 0.43$, $P = 9.9e\text{-}4$).

The peak region of 13q contains *POLR1D*, a subunit of both RNA polymerases I and III. RNA polymerase I is involved in the production of 18S, 5.8S, and 28S rRNAs, while RNA polymerase III synthesizes small essential RNAs, such as tRNAs, 5S rRNA, and some snRNAs (24). There is not much information regarding this gene in the literature. *POLR1D* is overexpressed in 42% of the primary tumors (> 2-fold), showing high correlation between expression and copy number ($r = 0.7, P = 8.6e\text{-}11$). Note that in (25) another gene, *CDK8*, located 1200 kb upstream *POLR1D*, was associated with this peak amplification.

We found 973 genes the expression of which differs between samples with low and high expression of *PMEPA1*. They were enriched by genes expressing proteins located in the oxidative phosphorylation pathway. Similar analyses were done for *POLR1D* and *CCDC68* (see Table S2).

Noncoding RNA. Some peak and focal CINons contain small noncoding RNA (Table 1). hsa-mir-103–2, identified on the (deleted) peak region of 20p13, was implicated in colon cancer and was found to be downregulated in tumors (26). The peak CINon on chromosome 15 is part of a region that is subjected to genomic imprinting, associated with Prader-Willi syndrome and Angelman syndrome (27). This peak region consists of 76 C/D snoRNAs, organized in 2 large clusters. Currently, these snoRNA are not known to be related to cancer. Another imprinted locus that consists of large clusters of C/D snoRNAs and microRNAs is located on 14q32 (27). Deletion of C/D snoRNAs could affect methylation of rRNAs or the function of core C/D box snoRNP. Additionally, chromosome 14q is among broad regions that were found to be deleted in colon cancer by others (3, 4) and also by us. Inactivation of imprinted regions requires the silencing of only 1 allele and therefore may serve as an efficient mechanism for inactivating TSGs.

Deriving Copy Number Changes from Expression Data. One of our principal aims was to search for associations between chromosomal events and clinically relevant features of the tumors, such as survival and progression. To enhance statistical power and reliability, this analysis must be based on as large a number of samples as possible. Because expression data are available for many more samples than are SNP data, it would be useful to impute copy number from expression (28, 29). To establish a reliable procedure, we constructed 2 chromosomal instability maps (see *Methods*), as shown in Fig. S1, for 45 aneuploid tumor samples, which had both expression and SNP data (see Table S3). To minimize variance because of small numbers of genes, we treated only broad CINons and the focal CINon of 1p (because it contained many probe sets). The similarity of the 2 maps is striking, and indeed, the correlations between the entries for each CINon were highly significant ($r > 0.6$ at 10% false discovery rate [FDR]). On the basis of these observations we built an expression-based CINon table (heat map) for all 256 adenoma and tumor samples for which we had expression data (including liver and lung metastasis); this table (heat map) is shown in Fig. 2*B* and serves as the basis of the analysis described below.

Association of Aberrations with Survival, Disease Progression, and Other Factors. We now searched for connections between the different aberrations of Fig. 2*B* and survival. As expected, there is strong correlation between clinical state and outcome in colon cancer patients: in our data, almost all stage 4 patients had poor outcome (either death of disease or recurrence within 60 months)

and almost all stage 1 and stage 2 patients had good outcome (status other than dead of disease, *and* recurrence-free interval of >60 months). To evaluate the potential additional value of a chromosome-based classification, we then used a Kaplan-Meier analysis to test for an association between each CINon and outcome (using the imputed CINons of Fig. 2). The lowest *p*-values (FDR ≤ 10%) belong to 8p, 4p, and 15q ($P = 0.008$, 0.011, 0.011, respectively; their Kaplan-Meier plots are shown in Fig. S2. Notably, deletions of chromosomal arms 8p and 4p have previously been related to poor prognosis (30, 31). These same chromosomal abnormalities were also highly correlated with clinical progression as determined by clinical stage 1–4 (P value = 0.0004, 0.0014, and 0.0027, respectively, at FDR ≤ 10% for 8p, 4p, and 15q, respectively). We next wished to learn whether an analysis of outcome in the context of chromosomal amplifications and deletions could provide additional prognostic value to that provided by clinical stage. If so, knowing the specific genes affected by these chromosomal changes could also provide insight into the mechanisms of tumor growth, spread, and resistance to treatment.

Therefore, we used the changes in copy numbers of chromosomal arms to develop a chromosome-based classification of the samples. In the resulting CINon matrices (Fig. 2), the primary tumors and adenomas were divided into 3 groups. Samples of group A (marked blue) have normal copy number of 18q (lost in 71% of the samples); group B (marked green) have deletions in 18q *and* in either 8p, 4p, or in 15q (but not in all); group C (red) samples have simultaneous deletions in 18q, 8p, 4p, and in 15q; group D (black) have metastases from liver and lung. Group A is composed mostly of adenomas and MIN tumors (see Fig. 2*B*), known to be mainly euploid (most of these patients had good outcome). Group B is composed of 18 poor and 40 good outcome samples. Group C contains 42 poor and 20 good outcome samples. The Kaplan-Meier plots of groups A + B versus group C is shown in Fig. 2 *C* and *D* for SNP and expression data, respectively. Whether chromosomal changes are measured in a small group of patients (SNP) or imputed in a larger group (expression) the results are very similar and suggest that coexisting deletions in 18q, 8p, 4p, and 15q is associated with a particularly poor prognosis.

Next we looked for association of the copy number change of each CINon with a variety of other clinical and molecular factors. We separated the samples into 2 groups on the basis of the factor tested (for example, clinical stage or *p53* mutation status) and used a *t* test (on the values from Fig. 2*B*) to evaluate CINon copy number differences between the 2 groups (at FDR ≤ 10%). Complete results are given in Table S4; here we highlight a few. The most significant copy number differences between adenoma and stage 1 tumors are associated with chromosomal arms 14q, 20q, 20p, and 8q ($P < 0.001$, FDR = 1%). Consistent with a previous publication (7), 20q amplification is the most frequent, affecting 91% of the tumors (Table 1) and it is even found in some adenomas.

Deletion of 22q was more frequent in stage 2 than stage 3 tumors. Mutant and wild-type *p53* samples were distinguished by many amplifications and deletions, the most significant ones being 20q, Xq, 13q, 17p, and 7q ($P < 0.001$). This is consistent with a view that the p53 mutation is an important step in facilitating chromosomal instability (refs. 5 and 32). Samples harboring mutant *kRAS* are more likely to display deletion of 20p, while those with a mutation in *APC* are more likely to have deletion of 18p. Examining the same SNP data, some of us found significant associations between *p53* mutation status and copy number changes of 20q, 13q, 20p, and 18q; as well as association of several chromosomal arms with *APC* mutation but not the association of 20p deletion with *kRAS* mutational status.

The Oxidative Phosphorylation Pathway Is Related to Survival. Finally, we sought particular molecular pathways that could be affected by the chromosomal amplifications or deletions that we showed to be related to prognosis. We focused on those genes that both mapped to regions affected by copy number change *and* the expression of which was highly correlated with the chromosomal change, i.e., the "correlated genes" described earlier. Employing the DAVID database (34, 35), we identified 15 pathways that were implicated by these chromosomal aberrations (FDR < 25%) (see Table S5).

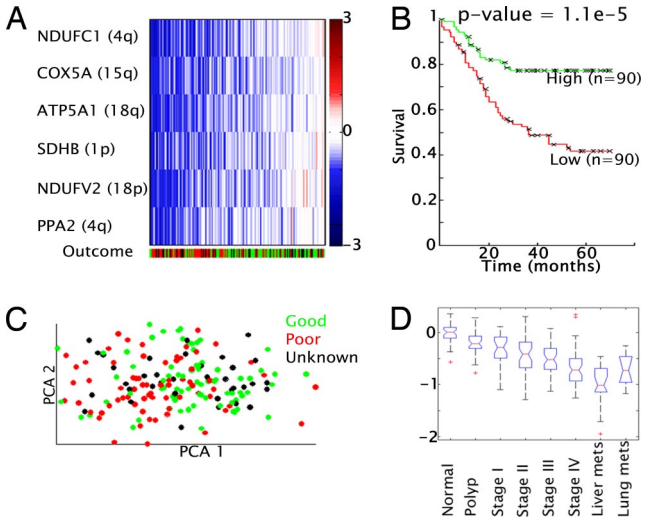

Fig. 3. The oxidative phosphorylation pathway. (*A*) Expression matrix of 6 genes belonging to the oxidative phosphorylation pathway, which were downregulated in poor outcome tumors. Primary tumor samples were ordered using SPIN (37), colored according to their outcome status; green represents good outcome, red poor outcome, and black represents unknown outcome. (*B*) Kaplan-Meier plot of 2 equal-sized groups of samples, partitioned according to the ordering in *a*. Follow-up intervals that were greater than 70 months were assigned 70. (*C*) First and second PCA plot of the primary tumor samples in the space of the 6 genes shown in *A*, using the same coloring. (*D*) Box plot of the mean log fold-change expression values of the 6 genes, grouped according to disease stages.

Oxidative phosphorylation was the only pathway that had significant association with survival: 23 of the 128 genes assigned by DAVID to oxidative phosphorylation were affected. Of these 23, 14 were downregulated and 9 were upregulated. Six genes are downregulated in the advanced stages of the disease (see Fig. 3 *A* and *D*). We used SPIN (36) to divide the samples into 2 groups on the basis of expression of these 6 genes (Fig. 3*A*). The Kaplan-Meier plot (Fig. 3*B*) exhibits significant separation of these 2 groups of samples (this was the only one of the 15 implicated pathways that yielded a significant Kaplan-Meier analysis (FDR ≤ 10%; $P < 0.01$). Fig. 3*C* shows the samples projected onto the first and second principal component analysis (PCA) from the space spanned by these 6 genes, showing a possible separation between good and poor outcome samples.

The oxidative phosphorylation pathway plays an intriguing role in cancer. In most nontransformed cells, 90% of ATP is produced in the mitochondria through oxidative phosphorylation, while 10% of ATP is attributed to anaerobic glycolysis. This ratio often shifts in tumor cells, where in some systems, more than 50% of the ATP is produced by glycolysis (37). These metabolic changes were identified over 70 years ago (38) and were explained by the hypoxic environment of the tumor. However, it is now understood that some neoplasms shift to glycolysis even under conditions of oxygen sufficiency (37).

HIF1 is a master transcriptional regulator of the adaptive response to hypoxia, which includes upregulation of genes responsible for glycolysis and downregulation of mitochondrial oxidative phosphorylation genes. Normally, the principal mechanism to activate *HIF1* is oxidative stress; however, other factors, such as activated oncogenes (*Ras*, *SRC*) or loss of TSGs (*VHL*, *PTEN*) can activate

HIF1 even under normoxic conditions (37, 39), as does accumulation of citric acid cycle constituents, succinate, or fumarate (37).

Several explanations have been proffered to explain this "glycolic shift": (*i*) the use of glycolytic metabolites such as ribose or citrate to enhance cell proliferation (37); (*ii*) high concentrations of lactate create an acidic environment that is advantageous to the process of invasion (40); (*iii*) decreased mitochondrial function reduces reactive oxygen species (ROS) production; however, the role of ROS in hypoxia-induced death is controversial (37); (*iv*) the shift to glycolysis also makes the tumor mitochondria less susceptible to permeabilization of the outer mitochondrial membrane, and as a result, less sensitive to apoptosis (40); and (*v*) the shift helps to conserve O_2 for alternative use such as sterol synthesis and oxidative protein folding (37). Our analysis indicates that one mechanism by which the neoplastic cell downregulates oxidative phosphorylation is deletion of the relevant genes and the resulting decrease in the activity of this pathway. This task of identifying all of the specific genes is challenging and not straightforward, perhaps because many different pathways converge on this essential cellular function. For example, based on the observation that *PTEN* loss results in *HIF1* accumulation (37), one might have anticipated an effect of *PTEN* loss on expression of oxidative phosphorylation genes. However, this was not observed (the mean *r* of *PTEN* expression with that of the genes in Fig. 3 was 0.13). Further insight may come from additional analysis of the different regulatory elements of this pathway, their status in the neoplastic cell, and the relations between them.

Methods

Expression Data. The 299 U133A arrays (see Table S3) were subjected to MAS 5, threshold, and log2 transformation (see *SI Methods* and Fig. S3). *Log-expression ratios* $ER_{n,s}$ were calculated by subtracting from the log-transformed expression value of probe set *n* in sample *s* the median log-transformed expression value of probe set *n* in the normal colon samples of the same batch (2 batches were identified, because of protocol change). For chromosome X, all normal samples of the same gender and batch were used.

SNP data are composed (see Table S3) of 130 50K XbaI SNP arrays (41). *Log-copy number ratios* $CR_{n,s}$ were calculated by subtracting from the log-transformed copy number of SNP *n* in sample *s* the log-transformed copy number of SNP *n* in the normal sample. The $CR_{n,s}$ values were smoothed with GLAD (33). See *SI Methods* for detailed normalization and preprocessing steps.

Identification of CINons. We used GISTIC (9). *Q*-values for the statistical significance of the copy number of each SNP were calculated for amplifications and deletions separately. CINons were then defined as regions of at least 5 contiguous SNPs with a *q*-value of <0.25 (for details see *SI Methods*). Two different configurations of GISTIC were used: *configuration 1* aimed at identifying all broad regions and *configuration 2* aimed at identifying small CINons (see *SI Methods*).

Correlation Between Expression and Copy Number. Detailed description is found in *SI Methods*. For each probe set *n*, the PCC was calculated between the $ER_{n,s}$ values of the samples that had both measures of expression and copy numbers (79 samples), and the copy number ratios measured in sample *s* from SNPs located near the probe set *n*. Each correlation was assigned with a *q*-value and FDR of 25% was then used to generate a list of "correlated genes."

CINon Expression Table. This analysis was limited to CINons that contained many probe sets—i.e., the broad CINons and the focal CINon of 1p. Using the "correlated genes," we constructed a CINon expression table; for each CINon *i* and sample *s* we calculated $CE_{i,s}$, the median ($ER_{n,s}$) evaluated for all probe sets *n* located on CINon *i*. A CINon copy number table was constructed in the same way, with entry $CC_{i,s}$ derived of CINon *i* and sample *s* by taking the median ($CR_{n,s}$) for all SNPs *n* that are located on CINon *i*. The CINon expression table may serve as a predictor of copy number for samples, for which no copy number data were available. To assess the quality of this prediction, PCCs of the $CE_{i,s}$ and $CC_{i,s}$ were calculated for each CINon *i* over the aneuploid tumor samples for which we had both expression and copy number measurements (45 samples, see Table S3 and Fig. S1).

ACKNOWLEDGMENTS. We thank G. Getz for help with implementation of GISTIC, and L. Hertzberg, and T. Shay for sharing their results. This work was funded by a Program Project Grant from the National Cancer Institute (P01-CA65930), a contract from the National Cancer Institute (263 MQ 610681), and by grants from the Ridgefield Foundation, the Ludwig Institute for Cancer Research/Conrad N. Hilton Foundation joint Hilton-Ludwig Cancer Metastasis Initiative, and the Gilbert Family Foundation.

1. Fearon ER, Vogelstein B (1990) A genetic model for colorectal tumorigenesis. *Cell* 61:759–767.
2. Lengauer C, Kinzler KW, Vogelstein B (1998) Genetic instabilities in human cancers. *Nature* 396:643–649.
3. Jones AM, et al. (2005) Array-CGH analysis of microsatellite-stable, near-diploid bowel cancers and comparison with other types of colorectal carcinoma. *Oncogene* 24:118–129.
4. Kurashina K, et al. (2008) Chromosome copy number analysis in screening for prognosis-related genomic regions in colorectal carcinoma. *Cancer Sci* 99:1835–1840.
5. Leslie A, et al. (2003) Mutations of APC, K-ras, and p53 are associated with specific chromosomal aberrations in colorectal adenocarcinomas. *Cancer Res* 63:4656–4661.
6. Albertson DG, Collins C, McCormick F, Gray JW (2003) Chromosome aberrations in solid tumors. *Nat Genet* 34:369–376.
7. Tsafrir D, et al. (2006) Relationship of gene expression and chromosomal abnormalities in colorectal cancer. *Cancer Res* 66:2129–2137.
8. Platzer P, et al. (2002) Silence of chromosomal amplifications in colon cancer. *Cancer Res* 62:1134–1138.
9. Beroukhim R, et al. (2007) Assessing the significance of chromosomal aberrations in cancer: Methodology and application to glioma. *Proc Natl Acad Sci USA* 104:20007–20012.
10. Ferrara N (2004) Vascular endothelial growth factor: Basic science and clinical progress. *Endocr Rev* 25:581–611.
11. Eswarakumar VP, Lax I, Schlessinger J (2005) Cellular signaling by fibroblast growth factor receptors. *Cytokine Growth Factor Rev* 16:139–149.
12. Goel A, et al. (2004) Frequent inactivation of PTEN by promoter hypermethylation in microsatellite instability-high sporadic colorectal cancers. *Cancer Res* 64:3014–3021.
13. Buffart TE, et al. (2005) DNA copy number changes at 8q11–24 in metastasized colorectal cancer. *Cell Oncol* 27:57–65.
14. Bates RC, Edwards NS, Burns GF, Fisher DE (2001) A CD44 survival pathway triggers chemoresistance via lyn kinase and phosphoinositide 3-kinase/Akt in colon carcinoma cells. *Cancer Res* 61:5275–5283.
15. Subramaniam V, et al. (2007) CD44 regulates cell migration in human colon cancer cells via Lyn kinase and AKT phosphorylation. *Exp Mol Pathol* 83:207–215.
16. Furge KA, Zhang YW, Vande Woude GF (2000) Met receptor tyrosine kinase: Enhanced signaling through adapter proteins. *Oncogene* 19:5582–5589.
17. Rundhaug JE (2005) Matrix metalloproteinases and angiogenesis. *J Cell Mol Med* 9:267–285.
18. Sala A (2005) B-MYB, a transcription factor implicated in regulating cell cycle, apoptosis and cancer. *Eur J Cancer* 41:2479–2484.
19. Wagner KW, et al. (2004) Overexpression, genomic amplification and therapeutic potential of inhibiting the UbcH10 ubiquitin conjugase in human carcinomas of diverse anatomic origin. *Oncogene* 23:6621–6629.
20. Katayama H, Brinkley WR, Sen S (2003) The Aurora kinases: Role in cell transformation and tumorigenesis. *Cancer Metastasis Rev* 22:451–464.
21. Gerhardt A, et al. (2004) Tissue expression and sero-reactivity of tumor-specific antigens in colorectal cancer. *Cancer Lett* 208:197–206.
22. Farrell C, et al. (2008) Somatic mutations to CSMD1 in colorectal adenocarcinomas. *Cancer Biol Ther* 7:609–613.
23. Hirokawa YS, et al. (2007) High level expression of STAG1/PMEPA1 in an androgen-independent prostate cancer PC3 subclone. *Cell Mol Biol Lett* 12:370–377.
24. Martinez-Calvillo S, et al. (2007) Characterization of the RNA polymerase II and III complexes in Leishmania major. *Int J Parasitol* 37:491–502.
25. Firestein R, et al. (2008) CDK8 is a colorectal cancer oncogene that regulates beta-catenin activity. *Nature* 455:547–451.
26. Cummins JM, et al. (2006) The colorectal microRNAome. *Proc Natl Acad Sci USA* 103:3687–3692.
27. Royo H, Bortolin ML, Seitz H, Cavaille J (2006) Small non-coding RNAs and genomic imprinting. *Cytogenet Genome Res* 113:99–108.
28. Carter SL, et al. (2006) A signature of chromosomal instability inferred from gene expression profiles predicts clinical outcome in multiple human cancers. *Nat Genet* 38:1043–1048.
29. Hertzberg L, et al. (2007) Prediction of chromosomal aneuploidy from gene expression data. *Genes Chromosomes Cancer* 46:75–86.
30. Al-Mulla F, et al. (2006) Metastatic recurrence of early-stage colorectal cancer is linked to loss of heterozygosity on chromosomes 4 and 14q. *J Clin Pathol* 59:624–630.
31. Bardi G, et al. (2004) Tumor karyotype predicts clinical outcome in colorectal cancer patients. *J Clin Oncol* 22:2623–2634.
32. Duensing A, Duensing S (2005) Guilt by association? p53 and the development of aneuploidy in cancer. *Biochem Biophys Res Commun* 331:694–700.
33. Hupe P, et al. (2004) Analysis of array CGH data: From signal ratio to gain and loss of DNA regions. *Bioinformatics* 20:3413–3422.
34. Dennis G, Jr., et al. (2003) DAVID: Database for annotation, visualization, and integrated discovery. *Genome Biol* 4:P3.
35. Hosack DA, et al. (2003) Identifying biological themes within lists of genes with EASE. *Genome Biol* 4:R70.
36. Tsafrir D, et al. (2005) Sorting points into neighborhoods (SPIN): Data analysis and visualization by ordering distance matrices. *Bioinformatics* 21:2301–2308.
37. Denko NC (2008) Hypoxia, HIF1 and glucose metabolism in the solid tumour. *Nat Rev Cancer* 8:705–713.
38. Warburg O (1956) On respiratory impairment in cancer cells. *Science* 124:269–270.
39. Bardos JI, Ashcroft M (2004) Hypoxia-inducible factor-1 and oncogenic signalling. *Bioessays* 26:262–269.
40. Gogvadze V, Orrenius S, Zhivotovsky B (2008) Mitochondria in cancer cells: What is so special about them? *Trends Cell Biol* 18:165–173.
41. Bacolod MD, et al. (2008) The signatures of autozygosity among patients with colorectal cancer. *Cancer Res* 68:2610–2621.